3-D Finite Element Analysis of Additional Eddy Current Losses in Induction Motors

Andrej Stermecki[1,2], Oszkár Bíró[1,2], Imam Bakhsh[1], Georg Ofner[3], Reinhard Ingruber[3]
1- Institute for Fundamentals and Theory in Electrical Engineering, Graz University of Technology
2- Christian Doppler Laboratory for Multiphysical Simulation, Analysis and Design of Electrical Machines
Kopernikusgasse 24, 8010 Graz, Austria
andrej.stermecki@tugraz.at
3- ELIN Motoren Gmbh, 8160 Preding/Weiz, Austria

Abstract —In this paper an approach based on the 3-D finite element (FE) analysis is proposed to evaluate additional eddy current losses in MW induction motors (IM). Losses produced by induced eddy currents in the end-region of the machine (stator clamping-plates and clamping-fingers) and losses provoked by parasitic leakage fields in the housing and in the metal parts of the cooling-ducts are investigated. Furthermore, additional losses produced by higher harmonic fields in the rotor squirrel cage are taken into consideration as well. Comprehensive 3-D FE models have been prepared in order to take these effects precisely into account. A numerical procedure based on non-conforming FE meshes has been used in order to simplify the modeling procedure and the solving process has been carried out in the frequency domain with the aim of reducing the computational time.

I. Introduction

Induced eddy currents in the inactive iron parts of the machine and induced spatial rotor current harmonics in the squirrel cage of the induction motors reduce the efficiency and contribute to overheating of electrical machines. This topic is especially prominent when MW induction motors are under investigation. In the design process, these parasitic effects can be minimized by using different materials (i.e. non magnetic steel) or by different designing strategies [1]. The losses produced by spatial rotor current harmonics in the squirrel cage can be reduced using an appropriate combination of stator and rotor slots and by optimization of the slot geometry [2], [3]. On the other hand, a computational estimation of these additional losses is a very demanding task and only rough estimations based on semi-empirical formulas are being used in the industry. Therefore, our efforts have been focused on developing a new numerical procedure for more accurate simulations of these phenomena.

II. Numerical Simulation and Preliminary Results

A. Losses in the end-region and in the cooling-ducts

A problem associated with FE simulations of the motor end-regions is the modeling process of the end-winding itself. To obtain a conforming FE mesh of the two layered windings and the surrounding air, an enormous number of FE is required which results in a huge computation time. Our method is based on non-conforming FE meshes with the FE mesh of the end-winding only used to perform a static current flow analysis. Such a mesh is relatively easy to obtain with the assistance of CAD programs. Knowing the current distribution in the end-winding, the Biot-Savart field is calculated in the integration points of another FE mesh representing the motor, its housing and the surrounding air. Since this second mesh is not conforming to the end-winding mesh (Fig. 1), preparing both models is not a very time-consuming task. In order to reduce the number of unknowns and consequently the computational time, the eddy current problem is solved in the frequency domain using the $\boldsymbol{T},\Phi\text{-}\Phi$ formulation [4]. Thus, the given current density $\boldsymbol{J}_0$ is represented by an arbitrary function $\boldsymbol{T}_0$, which satisfies the following condition:

$$curl(\boldsymbol{T}_0) = \boldsymbol{J}_0 \quad . \tag{1}$$

Knowing the numerically calculated Biot-Savart field $\boldsymbol{H}_s$, the rotational part $\boldsymbol{T}_0$ of the magnetic field is represented with the aid of edge element shape functions in order to avoid cancellation errors:

$$t_i = \int_{\text{Edge } i} \boldsymbol{H}_s \mathrm{d}l; \quad \boldsymbol{T}_0 = \sum_{\text{Edge } i}^{n_e} t_i \boldsymbol{N}_i \tag{2}$$

where $\boldsymbol{N}_i$ stands for the vectorial edge element basis functions associated with the i-th edge and n_e for the number of FE edges.

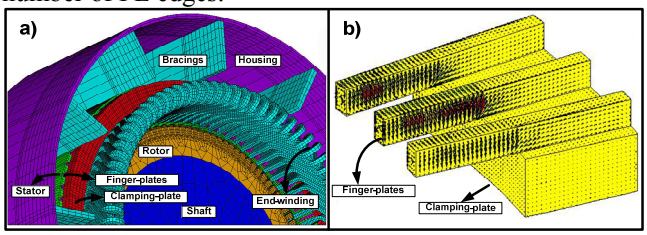

Fig. 1. a) 3-D model of the induction motor, b) Induced eddy currents in the part of the clamping-plate and clamping-fingers.

The preliminary results of these simulations show that the majority of the additional losses arise in the material adjacent to the current conductors (Fig. 1b and Table I).

TABLE I
ADDITIONAL LOSSES IN THE INACTIVE IRON PARTS

Current conducting volume	Calculated losses
Sum of all additional losses in the inactive iron parts	1 p.u.
Clamping fingers	0.57 p.u.
Clamping plates	0.27 p.u.
Metal parts in the cooling ducts	0.15 p.u.
Housing with bracings	0.01 p.u.

B. *Losses due to spatial rotor current harmonics*

The subject of this work is to compute the additional losses in the rotor squirrel cage under open-circuit conditions. It is sufficient to employ a 2-D numerical simulation based on the ***A***, ***A***-*V* formulation and with motion of the rotor taken into consideration in order to evaluate the copper losses in the rotor slots. The rotor movement has been realised using the time-stepping procedure where the geometry modification due to rotor rotation in every time-step has been considered by linear interpolation along the sliding interface in the air-gap [5]. The time increment between the two transient steps has been small enough to take the slot's harmonics into consideration:

$$\nu = p + gN_1; \quad g = \pm 1, \pm 2... \tag{3}$$

where ν denotes the spatial harmonic order, p stands for the number of stator pole pairs (p=7) and N_1 for the number of stator slots (N_1=84). These spatial harmonics induce the rotor currents with the rotor frequency (f_ν^R) of:

$$f_\nu^R = \left[\frac{f_\nu^S}{f_1} - (1-s)\frac{\nu}{p} \right] f_1 \tag{4}$$

where f_ν^S denotes the frequency of the spatial field wave in the stator coordinate system, s is the slip (s=0) and f_1 stands for the nominal frequency of 50 Hz. Hence, dominating rotor currents of frequencies of 300 Hz, 600 Hz, 1200 Hz and higher are to be expected. In order to discretize the current period of a frequency of 1200 Hz by 10 or more samples, the time-step of 50 μs has been employed.

Using this procedure the losses in rotor bars have been evaluated. The losses that arise in the short circuit ring, through which the rotor conductors are connected, can not be estimated by a 2D analysis. In order to evaluate these losses, a 3-D FE simulation has been additionally carried out. Since a transient 3-D analysis with the included motion would require an enormous amount of calculation time, the simulation has been carried out in the frequency domain. The model has been linearized and the superposition principle has been applied. By analyzing the harmonic content of the currents obtained by 2-D simulation, the individual rotor current harmonics have been separately prescribed to the 3-D model. As seen from Table II, using this proposed procedure, the losses in the rotor slots obtained by transient 2-D analysis and losses obtained by harmonic 3-D analysis are in good agreement. Based on these results the assumption can be made that the superposition principle is an acceptable method in order to reduce the computation time in the present work.

The 3-D simulation has been carried out using the ***A***, ***A***-*V* formulation in frequency domain. This formulation [6] has been additionally generalized in order to enable current excitation instead of the usual voltage excitation [7]. The separate harmonic content of the currents obtained by 2-D transient analysis has been prescribed to the 3-D model. In Fig. 2, the current distribution in the end-ring and in the rotor conductors is presented. Based on the findings of this investigation, the conclusion can be drawn that only a small fraction of the additional losses produced by spatial rotor current harmonics occur in the short circuit ring (only up to 1 %).

TABLE II
COMPARISON OF THE LOSSES OBTAINED BY TRANSIENT AND BY HARMONIC ANALYSES

Type of the analysis	**Calculated losses**
Harmonic analysis at 300 Hz	0.006 p.u.
Harmonic analysis at 600 Hz	0.968 p.u.
Harmonic analysis at 1200 Hz	0.008 p.u.
Sum of all losses obtained by harmonic analysis	**0.982 p.u.**
Transient analysis	**1 p.u.**

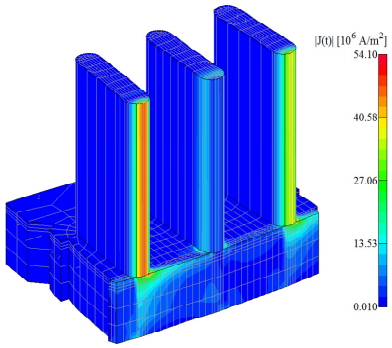

Fig. 2.The current distribution in the portion of the short-circuit ring.

ACKNOWLEDGMENT

This work has been supported by the Christian Doppler Research Association (CDG) and by the ELIN Motoren Gmbh.

III. REFERENCES

[1] R. Lin, A. Haavisto, and A. Arkkio, "Analysis of Eddy-Current Loss in End Shield and Frame of a Large Induction Machine," IEEE Trans. on Magn, vol. 46, no. 3, pp. 942-948, 2010.

[2] J. Germishuizen, A. Jöckel, and M. Kamper, "Numerical calculation of iron- and pulsation losses on induction machines with open stator slots," Proc. 16th Southern African Univ. Power Eng. Conf. (SAUPEC'07), University of Cape Town, South Africa, January 2007, on CD-ROM.

[3] J. Germishuizen and S. Stanton, "No Load Loss and Component Separation for Induction Machines," Proc. 18th Int. Conf. Electrical Machines (ICEM 2008), Rome, Italy, September 2008, pp. 1-5.

[4] O. Bíró, "Edge element formulations of eddy current problems," Computer Methods in Applied Mechanics and Engineering, vol. 169, pp. 391-405, 1999.

[5] R. Perrin-Bit and J. Coulomb, "A three-dimensional finite element mesh connection for problems involving movement," IEEE Trans. on Magn., vol. 31, no. 3, pp. 1920-1923, 1995.

[6] O. Bíró, P. Böhm, K. Preis, and G. Wachutka, "Edge Finite Element Analysis of Transient Skin Effect Problems", IEEE Trans. on Magn., vol. 36, no. 4, pp. 835 - 839, 2000.

[7] I. Bakhsh, O. Bíró, and K. Preis, "Skin Effect Problems with Prescribed Current Condition", 14th Int. IGTE Symposium on Numerical Field Calculation in Electrical Engineering, Graz, Austria, September 2010.